

Emphysematous pyonephrosis associated with extrahepatic portosystemic shunt in a dog

Jongsu LIM¹⁾, Youngmin YOON¹⁾, Dongin JUNG¹⁾, Seongchan YEON¹⁾ and Heechun LEE^{1)*}

¹⁾Institute of Animal Medicine, College of Veterinary Medicine, Gyeongsang National University, Jinju 660–701, Republic of Korea

(Received 26 March 2015/Accepted 28 November 2015/Published online in J-STAGE 12 December 2015)

ABSTRACT. A 16-month-old intact female Maltese dog was referred for examination of depression and vomiting. Ultrasonography revealed dilated right renal pelvis containing echogenic fluid with free gas. A hyperechoic material suspected of urolith was identified in the right ureter. Computed tomography revealed emphysematous change of the right kidney associated with ureteral obstruction and extrahepatic portosystemic shunt (EHPSS). Ureteronephrectomy and surgical correction were performed for the EHPSS. *Escherichia coli* was isolated from pus from the right kidney. Quantitative analysis revealed that the urolith was an ammonium urate stone. After 5 months follow-up, no complication was observed. This is the first report of emphysematous pyonephrosis associated with EHPSS in a dog.

KEY WORDS: ammonium urate, canine, portosystemic shunt, pyonephrosis

doi: 10.1292/jvms.15-0181; *J. Vet. Med. Sci.* 78(4): 697–700, 2016

Pyonephrosis defined as infected hydronephrosis associated with suppurative destruction of the parenchyma of the kidney may cause septic shock [6, 18]. Almost all dogs with pyonephrosis have conspicuous obstruction in the renal collecting system [5, 13, 20]. Animals with portosystemic shunt (PSS) may show urinary tract signs. These signs can be associated with ureteral obstruction caused by ammonium urate urolith and bacterial upper urinary tract infections (UTIs) [7, 14, 17]. Here, we report emphysematous pyonephrosis associated with PSS in a dog.

A 16-month-old intact female Maltese was referred for examination of depression and vomiting within an hour after eating high-protein food. Its rectal temperature was 39.8°C. No other abnormality was noted on physical examination. Complete blood cell counts (CBC) showed anemia (hematocrit 25%, reference 37–55%), leukocytosis ($27.06 \times 10^9/l$, reference $0.6\text{--}17.0 \times 10^9/l$) and thrombocytopenia ($134 \times 10^9/l$, reference $200\text{--}500 \times 10^9/l$). On biochemical profiling, the following abnormalities were noted: elevated alkaline phosphate (994 U/l, reference 20–150 U/l), hypoalbuminemia (1.8 g/dl, reference 2.5–4.4 g/dl) and hypoglycemia (38 mg/dl, reference 74–143 mg/dl). Serum urea nitrogen level and creatinine level were within the normal range. Serum bile acid (SBA) was elevated over 30 $\mu\text{mol/l}$ on preprandial (reference 0.2–4.3 $\mu\text{mol/l}$) and two-hour postprandial (reference 0.6–24.2 $\mu\text{mol/l}$). Urinalysis showed proteinuria (protein level of 2+), glycosuria (glucose level of 1+) and normal urine specific gravity (1.025) with dipstick analysis. There were rod-shaped bacteria and neutrophils in the urine

aspirated on sediment examination with Diff-Quick stain.

On radiographs, right-sided renomegaly and microhepatica were identified. A well-defined round shaped gas opacity was superimposed with enlarged right kidney (Fig. 1). On ultrasonography (Xario SSA-660A, Toshiba Medical Systems Corp., Otawara, Japan), the right renal pelvis was dilated containing echogenic fluid. Reverberation and bright speckles with dirty shadowing were found just below the medial interface of the diverticuli consistent with free gas (Fig. 1). An 18.1 mm-wide spindle-shaped and hyperechoic structure with distal shadowing was identified. It was consistent with cranial ureteral dilation. Urinary bladder was thickened irregularly. It was filled with echogenic sludge. Its liver was diffusely hyperechoic. The main portal vein was small in diameter. The extrahepatic portal flow was reduced. A dual-phase computed tomographic angiogram (CTA) was performed (Somatom Emotion, Siemens, Muenchen, Germany). Iodinated contrast medium (Omnipaque, GE healthcare, Cork, Ireland) was administered (814 mgI/kg) at 1 ml/sec into a cephalic vein by an automatic angiographic injector (CT 9000ADV, Liebel-Flarsheim, Cincinnati, OH, U.S.A.). Images were acquired from the start of arterial phase at 12 sec and portal phase at 33 sec after administering the contrast medium in compliance of a previous study [26]. The shunting vessel arose from the gastroduodenal vein and extended ventrally leftward and cranially along the lesser curvature of the stomach. It passed cranial to the liver along the diaphragm and connected to the caudal vena cava from the left side via the phrenic vein (Fig. 2). Right kidney was filled with non-enhancing content with a small amount of gas (Fig. 2). Calculi were identified in the right ureter and the left renal pelvis. Based on these findings, emphysematous pyonephrosis with a congenital extrahepatic portosystemic shunt (EHPSS) was the tentative diagnosis.

Ureteronephrectomy revealed that the renal pelvis was filled with a large amount of dark brown-colored pus. A yellowish green, $5.8 \times 3.2 \times 4.2$ mm sized, and pyramidal-

*CORRESPONDENCE TO: LEE, H., College of Veterinary Medicine, Gyeongsang National University, Jinju 660–701, Republic of Korea. e-mail: lhc@gnu.ac.kr

©2016 The Japanese Society of Veterinary Science

This is an open-access article distributed under the terms of the Creative Commons Attribution Non-Commercial No Derivatives (by-nc-nd) License <<http://creativecommons.org/licenses/by-nc-nd/4.0/>>.

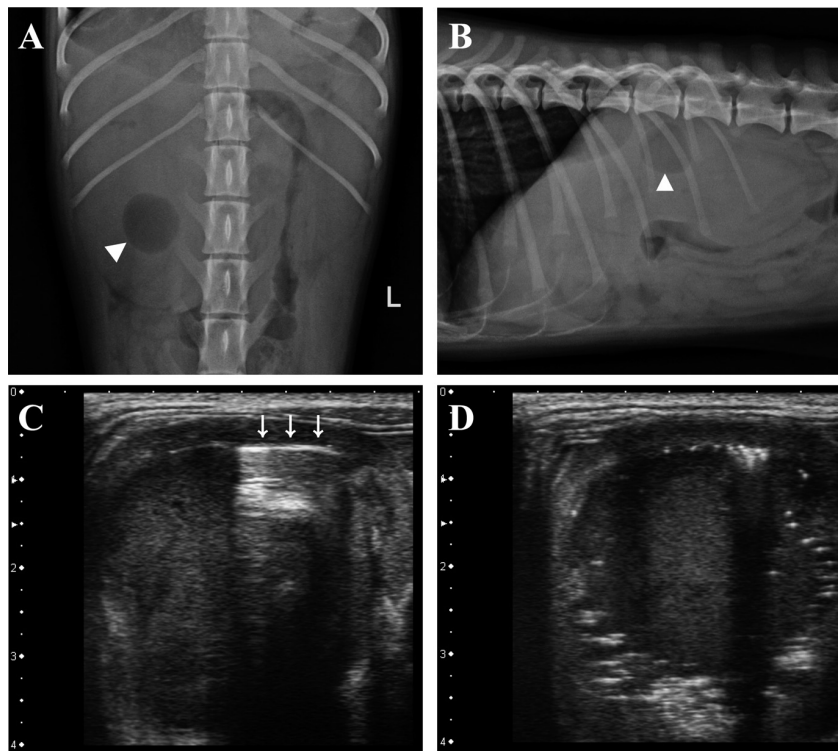


Fig. 1. Ventrodorsal view (A) and right lateral view (B) of abdominal radiographs showing gas opacity (arrowhead) superimposed on enlarged right kidney. Small intestine in cranial abdomen is displaced ventrally to kidney with microhepatica (B). A reverberation artifact (C, arrows) and bright speckles with distal acoustic shadowing (D) existed internally interfacing the diverticuli.

shaped calculus was presented in the right ureter (Fig. 3). Surgical correction of the EHPSS was performed around the shunt close to the caudal vena cava using surgically placed cellophane bands. *Escherichia coli* was isolated from the pus. Quantitative analysis of the urolith revealed 50% ammonium acid urate and 50% non-urolithic materials. After the surgical procedure, clinical signs were resolved. At follow-up of 5 months, no complication was observed.

Ammonium acid urate calculi are common in PSS patients. They can be associated with bacterial upper urinary tract infections [14, 17]. Patients with PSS often show hematologic changes, including nonregenerative anemia, leukocytosis, hypoalbuminemia, hypocholesterolemia, hypoglycemia and elevated serum liver enzyme [8, 24]. Although normal Maltese dogs have been reported to have elevated SBA, increases in postprandial SBA are sensitive markers to detect PSS in dogs [1–3, 8, 23]. In this case, ammonia tolerance test was excluded, because all clinical signs and hematologic changes indicated that the patient might have PSS. Septicemia was also suspected due to suppurative destruction of the right kidney consistent with hematologic abnormalities.

If the kidney is unilaterally enlarged on radiography, hydronephrosis, renal tumor and subcapsular hematoma or abscess could be considered [22]. Although ureteral calculi are often radiopaque, urate stones are usually radiolucent [22].

According to previous reports, almost all dogs with pyonephrosis have conspicuous obstruction in the renal collecting system [5, 13, 20]. In this case, the right kidney was dilated with pus due to urinary obstruction by urate stone and UTIs. In addition, the pyramidal shape of the stone suggested that urolith could have formed in the renal pelvis and dislodged into the ureter. Imaging for the portal and hepatic vasculature is essential for diagnosis of PSS in a dog. Dual-phase CTA is a minimally invasive imaging modality. It provides excellent anatomic details of the hepatic and portal vasculature [26]. In this case, dynamic scan was not performed, because we were concerned about the nephrotoxicity related to iodinated contrast media [15]. Based on available literatures, this case was similar to right gastric-phrenic type [9, 11, 16, 21].

In animals with PSS, urinary disorders can be associated with bacterial UTIs [12, 14]. Detection of bacteria on urine sediment examination can strongly suggest bacterial UTIs [19]. Rod-shaped bacteria and neutrophils were identified in this case. Based on available literatures, *E. coli* is the most common offending organism in the kidney of dogs [12]. Although emphysematous change of kidney is usually associated with *E. coli* in humans, it has been discussed in dogs only in a few cases [4, 10, 12, 13, 20, 25]. In this case, free gas was identified in the right kidney, and *E. coli* was isolated from the pus in the right renal collecting system.

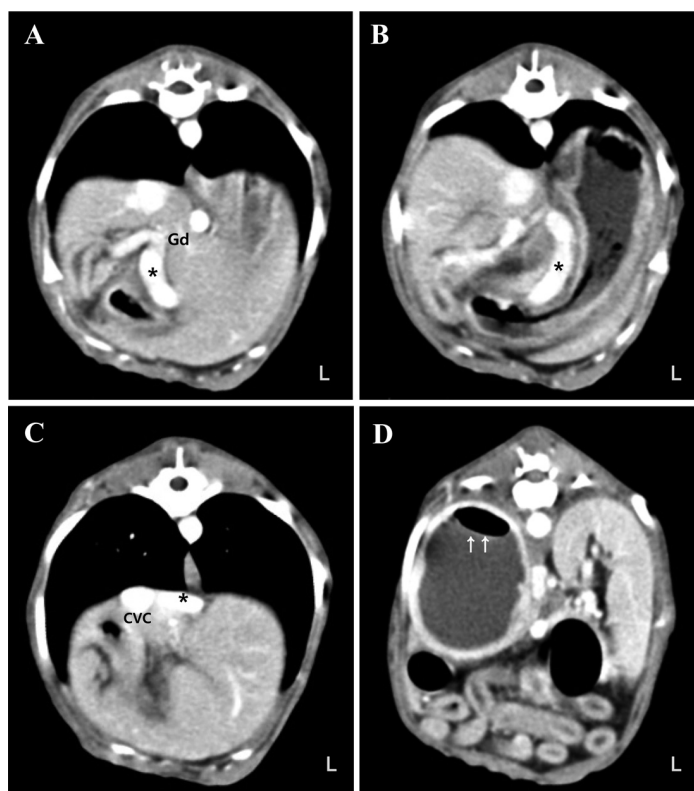


Fig. 2. Computed tomographic angiogram of the abdomen. The shunting vessel (asterisk) arised from the gastroduodenal vein (Gd) and extended ventrally (A), leftward and cranially along the lesser curvature of the stomach (B). It passed cranially to the liver along the diaphragm and connected to the caudal vena cava (CVC) from the left side via the phrenic vein (C). A small amount of gas (arrows) existed in the right kidney (D).

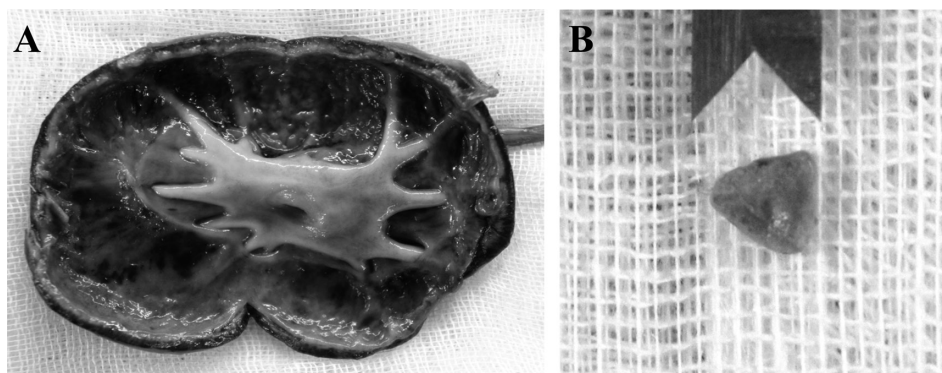


Fig. 3. Dorsal section of right kidney (A). Dilated renal pelvis with a destruction of the parenchyma is marked. A pyramidal-shaped calculus is in the right ureter (B).

Emphysematous pyonephrosis with EHPSS is very rare in veterinary medicine, although a similar case has reported that ammonium urate urolith has resulted in hydronephrosis in a PSS dog [7]. In this case, more severe progression with obstructive lesion and UTIs complicated with suppurative and emphysematous change was found compared to the

previous report. In addition, we cultured the bacteria and identified the causative organism.

In most cases, clinicians may consider UTIs and/or ureteral obstruction, if emphysematous and purulent change of kidney is identified. However, it is possible that the causes of obstructive ureter stone, such as EHPSS, are overlooked

due to the severity of clinical symptoms. Therefore, detailed investigation using US and CT should be considered for cases with obstructive ureter stones. This report is unique due to the severe progression of pyonephrosis. To the best of our knowledge, this is the first report of emphysematous pyonephrosis associated with congenital PSS in a dog.

REFERENCES

- Center, S. A., Erb, H. N. and Joseph, S. A. 1995. Measurement of serum bile acids concentrations for diagnosis of hepatobiliary disease in cats. *J. Am. Vet. Med. Assoc.* **207**: 1048–1054. [[Medline](#)]
- Center, S. A., ManWarren, T., Slater, M. R. and Wilentz, E. 1991. Evaluation of twelve-hour preprandial and two-hour postprandial serum bile acids concentrations for diagnosis of hepatobiliary disease in dogs. *J. Am. Vet. Med. Assoc.* **199**: 217–226. [[Medline](#)]
- Center, S. A. 1993. Serum bile acids in companion animal medicine. *Vet. Clin. North Am. Small Anim. Pract.* **23**: 625–657. [[Medline](#)] [[CrossRef](#)]
- Choi, J., Jang, J., Choi, H., Kim, H. and Yoon, J. 2010. Ultrasonographic features of pyonephrosis in dogs. *Vet. Radiol. Ultrasound* **51**: 548–553. [[Medline](#)] [[CrossRef](#)]
- Christiansen, J. S., Hottinger, H. A., Allen, L., Phillips, L. and Aronson, L. R. 2000. Hepatic microvascular dysplasia in dogs: a retrospective study of 24 cases (1987–1995). *J. Am. Anim. Hosp. Assoc.* **36**: 385–389. [[Medline](#)] [[CrossRef](#)]
- Coleman, B. G., Arger, P. H., Mulhern, C. B. Jr., Pollack, H. M. and Banner, M. P. 1981. Pyonephrosis: sonography in the diagnosis and management. *AJR Am. J. Roentgenol.* **137**: 939–943. [[Medline](#)] [[CrossRef](#)]
- da Silva Curiel, J. M., Pope, E. R., O'Brien, D. P. and Schmidt, D. A. 1990. Ammonium urate urolith resulting in hydronephrosis and hydroureter in a dog with a congenital portosystemic shunt. *Can. Vet. J.* **31**: 116–117. [[Medline](#)]
- Ettinger, S. J. and Feldman, E. C. 2009. Liver and pancreatic diseases. pp. 1649–1654. *In: Textbook of Veterinary Internal Medicine*, 7th ed. (Duncan, L., Rudolph, P. and Harms, L. eds.), Saunders, St. Louis.
- Fukushima, K., Kanemoto, H., Ohno, K., Takahashi, M., Fujiwara, R., Nishimura, R. and Tsujimoto, H. 2014. Computed tomographic morphology and clinical features of extrahepatic portosystemic shunts in 172 dogs in Japan. *Vet. J.* **199**: 376–381. [[Medline](#)] [[CrossRef](#)]
- Huang, J. J. and Tseng, C. C. 2000. Emphysematous pyelonephritis: clinicoradiological classification, management, prognosis, and pathogenesis. *Arch. Intern. Med.* **160**: 797–805. [[Medline](#)] [[CrossRef](#)]
- Kraun, M. B., Nelson, L. L., Hauptman, J. G. and Nelson, N. C. 2014. Analysis of the relationship of extrahepatic portosystemic shunt morphology with clinical variables in dogs: 53 cases (2009–2012). *J. Am. Vet. Med. Assoc.* **245**: 540–549. [[Medline](#)] [[CrossRef](#)]
- Ling, G. V., Norris, C. R., Franti, C. E., Eisele, P. H., Johnson, D. L., Ruby, A. L. and Jang, S. S. 2001. Interrelations of organism prevalence, specimen collection method, and host age, sex, and breed among 8,354 canine urinary tract infections (1969–1995). *J. Vet. Intern. Med.* **15**: 341–347. [[Medline](#)]
- Madewell, B. R., Creed, J. E. and Hopkins, J. B. 1975. Hydronephrosis and pyelonephritis in a dog. *J. Am. Vet. Med. Assoc.* **167**: 377–379. [[Medline](#)]
- Marretta, S. M., Pask, A. J., Greene, R. W. and Liu, S. 1981. Urinary calculi associated with portosystemic shunts in six dogs. *J. Am. Vet. Med. Assoc.* **178**: 133–137. [[Medline](#)]
- Morcos, S. K. and Thomsen, H. S. 2001. Adverse reactions to iodinated contrast media. *Eur. Radiol.* **11**: 1267–1275. [[Medline](#)] [[CrossRef](#)]
- Nelson, N. C. and Nelson, L. L. 2011. Anatomy of extrahepatic portosystemic shunts in dogs as determined by computed tomography angiography. *Vet. Radiol. Ultrasound* **52**: 498–506. [[Medline](#)] [[CrossRef](#)]
- Nelson, R. W. and Couto, C. G. 2009. Hepatobiliary and exocrine pancreatic disorders. pp. 535–537. *In: Small Animal Internal Medicine*, 4th ed. (Duncan, L., and Winkel, A. eds.), Mosby, St. Louis.
- Subramanyam, B. R., Raghavendra, B. N., Bosniak, M. A., Lefleur, R. S., Rosen, R. J. and Horii, S. C. 1983. Sonography of pyonephrosis: a prospective study. *AJR Am. J. Roentgenol.* **140**: 991–993. [[Medline](#)] [[CrossRef](#)]
- Swenson, C. L., Boisvert, A. M., Kruger, J. M. and Gibbons-Burgener, S. N. 2004. Evaluation of modified Wright-staining of urine sediment as a method for accurate detection of bacteriuria in dogs. *J. Am. Vet. Med. Assoc.* **224**: 1282–1289. [[Medline](#)] [[CrossRef](#)]
- Szatmári, V., Ösi, Z. and Manczur, F. 2001. Ultrasound-guided percutaneous drainage for treatment of pyonephrosis in two dogs. *J. Am. Vet. Med. Assoc.* **218**: 1796–1799, 1778–1779. [[Medline](#)] [[CrossRef](#)]
- Szatmári, V., van Sluijs, F. J., Rothuizen, J. and Voorhout, G. 2004. Ultrasonographic assessment of hemodynamic changes in the portal vein during surgical attenuation of congenital extrahepatic portosystemic shunts in dogs. *J. Am. Vet. Med. Assoc.* **224**: 395–402. [[Medline](#)] [[CrossRef](#)]
- Thrall, D. E. 2013. The abdominal cavity: canine and feline. pp. 711–730. *In: Textbook of Veterinary Diagnostic Radiology*, 6th ed. (Duncan, L. ed.), Saunders, St. Louis.
- Tisdall, P. L. C., Hunt, G. B., Bellenger, C. R. and Malik, R. 1994. Congenital portosystemic shunts in Maltese and Australian cattle dogs. *Aust. Vet. J.* **71**: 174–178. [[Medline](#)] [[CrossRef](#)]
- Tobias, K. M. and Besser, T. E. 1997. Evaluation of leukocytosis, bacteremia, and portal vein partial oxygen tension in clinically normal dogs and dogs with portosystemic shunts. *J. Am. Vet. Med. Assoc.* **211**: 715–718. [[Medline](#)]
- Wong, Y., Suh, B., Parsons, R., Telivala, B., Haas, N., Chen, D. and Greenberg, R. 2009. Emphysematous pyelonephritis caused by *Pasteurella multocida*. *Infect. Med.* **26**: 60.
- Zwingerberger, A. L. and Schwarz, T. 2004. Dual-phase CT angiography of the normal canine portal and hepatic vasculature. *Vet. Radiol. Ultrasound* **45**: 117–124. [[Medline](#)] [[CrossRef](#)]